Int. J. Adv. Appl. Math. and Mech. 8(1) (2020) 40 – 49 (ISSN: 2347-2529)

Journal homepage: www.ijaamm.com

IJAAMM

International Journal of Advances in Applied Mathematics and Mechanics

Second order chemical reaction on MHD flow past a vertical porous plate with Soret and Dufour effects

Research Article

A.K. Shukla*, **Yogendra Kumar Dwivedi**

Department of Mathematics RSKD PG College Jaunpur-222001, India

Received 23 April 2020; accepted (in revised version) 27 May 2020

Abstract: In This paper, we investigate the changes of Soret and Dufour effects on MHD (magnetohydrodynamics) flow past a vertical porous plate with second-order chemical reaction. The governing equations of motion are the system of partial differential equations, these equations are nondimensionalized by introducing nondimensional physical quantities. Nondimensional partial differential equations flow are solved numerically using the Crank-Nicolson finite difference method. The skin friction, Nusselt number and Sherwood number, as well as some effects of different parameters on velocity, temperature and concentration profiles are studied through graphs and tables.

MSC: 76W05 • 80A20 • 80A21 • 80A32 • 80M20

Keywords: Magnetohydrodynamics • Heat Transfer • Mass Transfer • Order of chemical reaction • Soret and Dufour effects • Crank-Nicolson finite difference method

1. Introduction

A large number of mathematicians has been given attention towards unsteady MHD flow past a vertical porous plate with Soret-Dufour and second-order chemical reaction. The investigation of the effect of mass transfer on Newtonian and Non-Newtonian fluids has become important in the last few years. The heat transfer by radiation has many applications in the different fields like the design of engines and combustion chambers to operate at increased temperature to raise thermal efficiency, Solar energy, semiconductor water processing, manufacturing of transient crystals, energy transfer in furnaces, etc. Nadeem et al.[1] has investigated the effects of thermal radiation on nano-fluid towards a stretching sheet with convective boundary conditions. Ibrahim et al.[2] projected their aim on Williamson nano-fluid flow in the presence of thermal radiation.

Oztop and Selimefendegin[3] employed the finite element method to find out a numerical solution of MHD mixed convection in a flexible-walled and nanofluid filled the lid-derived cavity with volumetric heat generation. Kumar and Rajput[4] investigated the effect of radiation on MHD flow past an impulsively started vertical plate with variable heat and mass transfer. Ahmad et al.[5].

Kharabela et al.[7] worked on higher-order chemical reactions on MHD nanofluid flow with slip boundary conditions. Matta and Gajjela [8] have analysed the order of chemical reaction and convective boundary conditions on effects on micropolar fluid over a stretching sheet. Usman et al.[9] studied MHD free convective flow with thermal radiation and chemical reaction effects in the presence of variable suction. Rahman [10] explored the combined effect of

* Corresponding author.

E-mail address(es): ashishshukla1987@gmail.com (A.K. Shukla).

internal heat generation and higher-order chemical reaction on the non-Dercian forced convective flow of a viscous incompressible fluid with variable viscosity and thermal conductivity over a stretching surface embedded in a porous medium.

Motivating from the above research work and the various possible industrial applications of the engineering fields. It is a great interest in the investigation of unsteady MHD flow through a vertical porous plate with Soret-Dufour and second-order chemical reaction. The effect of different parameters on velocity, temperature, mass transfer, shearing stress, local surface heat, and mass flux are received by solving numerically using Crank-Nicolson finite difference method the governing equations of flow field and effects of appropriate parameters.

2. Mathematical Model

Electrically conducting boundary layer flow of viscous incompressible fluid over a permeable vertical plate immersed in a porous medium has been considered. Let us consider the plate gets heated at temperature $\tilde{T}_w$ and concentration $\tilde{C}_w$. In this model Soret-Dufour effects and second-order chemical reaction in flow variable is taken into account. The plate is considered infinite in $\tilde{x}$-direction and $\tilde{y}$-axis normal to the plate. $\frac{\partial \tilde{u}}{\partial \tilde{x}}$ is negligible in equation of continuity because flow direction is vertically upward.

In starting, $\tilde{t} \leq 0$ we assumed that the plate and fluid are at the same temperature and concentration. For $\tilde{t} > 0$, the plate moves with velocity u_0 and concentration and temperature increase exponentially with time. The induced magnetic field is neglected because transversely applied magnetic field and magnetic Reynold's number are small. In the direction of $\tilde{y}$-axis, a magnetic field of uniform strength B_0 is considered.

According to usual Boussinesq's approximation the governing equations and boundary conditions of this model are given as:

$$\frac{\partial \tilde{v}}{\partial \tilde{y}} = 0 \Rightarrow \tilde{v} = -v_0 (constant) \tag{1}$$

$$\frac{\partial \tilde{u}}{\partial \tilde{y}} + \tilde{v}\frac{\partial \tilde{u}}{\partial \tilde{y}} = \nu \frac{\partial \tilde{u}}{\partial \tilde{y}^2} + g\beta_t(\tilde{T} - \tilde{T}_\infty) + g\beta_c(\tilde{C} - \tilde{C}_\infty) - \frac{\sigma B_0^2 \tilde{u}}{\rho} - \frac{\nu \tilde{u}}{\tilde{K}} \tag{2}$$

$$\rho c_p \left(\frac{\partial \tilde{T}}{\partial \tilde{t}} + \tilde{v}\frac{\partial \tilde{T}}{\partial \tilde{y}} \right) = k\frac{\partial^2 \tilde{T}}{\partial \tilde{y}^2} - \frac{\partial q_r}{\partial \tilde{y}} + \frac{\rho D_m K_T}{c_s}\frac{\partial^2 \tilde{C}}{\partial \tilde{y}^2} \tag{3}$$

$$\frac{\partial \tilde{C}}{\partial \tilde{t}} + \tilde{v}\frac{\partial \tilde{C}}{\partial \tilde{y}} = D\frac{\partial^2 \tilde{C}}{\partial \tilde{y}^2} + \frac{D_m K_T}{T_m}\frac{\partial^2 \tilde{T}}{\partial \tilde{y}^2} - k_r(\tilde{C} - \tilde{C}_\infty)^2 \tag{4}$$

where $\tilde{T}$ and $\tilde{C}$ are dimensional temperature and concentration , $\tilde{C}_\infty$ and $\tilde{T}_\infty$ are concentration and temperature of free stream, in equation 4; $k_r(\tilde{C} - \tilde{C}_\infty)^2$ has come on account of second order chemical reaction, k_r is chemical reaction constant, β_t is volumetric coefficient of thermal expansion, β_c is coefficient of volume expansion for mass transfer, q_r is radiative heat along $\tilde{y}$-axis, ν is kinematic viscosity and T_m is mean fluid temperature, $\tilde{v}$ is suction velocity along $\tilde{y}$-axis, $\tilde{K}$ is permeability of porous medium, σ is electrical conductivity, D_m is molecular diffusivity, g is acceleration due to gravity, K_T is thermal diffusion ratio, μ is viscosity, ρ is fluid density, k is thermal conductivity of fluid, c_p is specific heat at constant pressure,

The boundary conditions for this model are assumed as:

$$\begin{aligned} &\tilde{t} \leq 0 \quad \tilde{u} = 0 \quad \tilde{T} = \tilde{T}_\infty \quad \tilde{C} = \tilde{C}_\infty \quad \forall\ \tilde{y} \\ \tilde{t} > 0 \quad &\tilde{u} = u_0 \quad \tilde{v} = -v_0 \quad \tilde{T} = \tilde{T}_\infty + (\tilde{T}_w - \tilde{T}_\infty)e^{-A\tilde{t}}, \\ &\tilde{C} = \tilde{C}_\infty + (\tilde{C}_w - \tilde{C}_\infty)e^{-A\tilde{t}}, \quad at\ \tilde{y} = 0 \\ &\tilde{u} = 0 \quad \tilde{T} \to \tilde{T}_\infty \quad \tilde{C} \to \tilde{C}_\infty \quad \tilde{y} \to \infty \end{aligned} \tag{5}$$

where $\tilde{T}_w$ and $\tilde{C}_w$ are concentration and temperature respectively of plate and $A = \frac{v_0^2}{\nu}$.

The radiative heat flux term by using the Roseland approximation is given by

$$q_r = -\frac{4\sigma}{3k_m}\frac{\partial \tilde{T}^4}{\partial \tilde{y}} \tag{6}$$

where k_m is the mean absorption coefficient and σ is Stefan Boltzmann constant. In this problem, $\tilde{T}^4$ may be expressed linearly with temperature because temperature difference within a flow is very small. It is seen by expanding in a Taylor's series about $\tilde{T}_\infty$ and considering the negligible higher-order term, so

$$\tilde{T}^4 \cong 4\tilde{T}_\infty^3 \tilde{T} - 3\tilde{T}_\infty^4 \tag{7}$$

so, with the help of equations 6 and 7, equation 3 is reduced to

$$\rho c_p \left(\frac{\partial \tilde{T}}{\partial \tilde{t}} + \tilde{v}\frac{\partial \tilde{T}}{\partial \tilde{y}}\right) = k\frac{\partial^2 \tilde{T}}{\partial \tilde{y}^2} + \frac{16\sigma \tilde{T}_\infty^3}{3k_m}\frac{\partial^2 \tilde{T}}{\partial \tilde{y}^2} + \frac{\rho D_m K_T}{c_s}\frac{\partial^2 \tilde{C}}{\partial \tilde{y}^2} \tag{8}$$

To nondimensional form of governing equations, we employ the following quantities:

$$\begin{aligned} &u = \frac{\tilde{u}}{u_0},\ t = \frac{\tilde{t}v_0^2}{\nu},\ \theta = \frac{\tilde{T}-\tilde{T}_\infty}{\tilde{T}_w-\tilde{T}_\infty},\ C = \frac{\tilde{C}-\tilde{C}_\infty}{\tilde{C}_w-\tilde{C}_\infty},\ Gm = \frac{\nu g\beta_c(\tilde{C}_w-\tilde{C}_\infty)}{u_0 v_0^2},\\ &Gr = \frac{\nu g\beta_t(\tilde{T}_w-\tilde{T}_\infty)}{u_0 v_0^2},\ Du = \frac{D_m K_T(\tilde{C}_w-\tilde{C}_\infty)}{c_s c_p \nu(\tilde{T}_w-\tilde{T}_\infty)},\ Sr = \frac{D_m K_T(\tilde{T}_w-\tilde{T}_\infty)}{T_m \nu(\tilde{C}_w-\tilde{C}_\infty)},\\ &K = \frac{v_0^2\tilde{K}}{\nu^2,},\ Pr = \frac{\mu c_p}{k},\ M = \frac{\sigma B_0^2 \nu}{\rho v_0^2},\ R = \frac{4\sigma \tilde{T}_\infty^3}{k_m k},\ Sc = \frac{\nu}{D_m},\ y = \frac{\tilde{y}v_0}{\nu},\ K_r = \frac{k_r \nu}{v_0^2}. \end{aligned} \tag{9}$$

Using substitutions of equation 9, we get non-dimensional form of partial differential equations 2, 8 and 4 respectively:

$$\frac{\partial u}{\partial t} - \frac{\partial u}{\partial y} = \frac{\partial^2 u}{\partial y^2} + Gr\,\theta + Gm\,C - \left(M + \frac{1}{K}\right)u \tag{10}$$

$$\frac{\partial \theta}{\partial t} - \frac{\partial \theta}{\partial y} = \frac{1}{Pr}\left(1 + \frac{4R}{3}\right)\frac{\partial^2 \theta}{\partial y^2} + Du\frac{\partial^2 C}{\partial y^2} \tag{11}$$

$$\frac{\partial C}{\partial t} - \frac{\partial C}{\partial y} = \frac{1}{Sc}\frac{\partial^2 C}{\partial y^2} + Sr\frac{\partial^2 \theta}{\partial y^2} - K_r C^2 \tag{12}$$

with boundary conditions

$$\begin{aligned} &t \le 0 \quad u = 0 \quad \theta = 0 \quad C = 0 \quad \forall\ y\\ &t > 0 \quad u = 1 \quad \theta = e^{-t} \quad C = e^{-t} \quad at\ y = 0\\ &\qquad u = 0 \quad \theta \to 0 \quad C \to 0 \quad y \to \infty. \end{aligned} \tag{13}$$

It is important to calculate the physical parameters for primary interest of this type boundary layer flow

$$\begin{aligned} \tau &= \left(\frac{\partial u}{\partial y}\right)_{y=0}\\ Nu &= -\left(\frac{\partial \theta}{\partial y}\right)_{y=0}\\ Sh &= -\left(\frac{\partial C}{\partial y}\right)_{y=0} \end{aligned} \tag{14}$$

3. Numerical Method of Solution

Exact solution of system of partial differential equations 10, 11 and 12 with boundary conditions 13 are impossible. So, these are solved using Crank-Nicolson implicit finite difference method. The Crank-Nicolson implicit finite difference method is a second order method $\left(o\left(\Delta t^2\right)\right)$ in time and has no restriction on space and time steps, that is, the method is unconditionally stable. The computation is executed for $\Delta y = 0.1$, $\Delta t = 0.001$ and procedure is repeated till $y = 4$. Equations 10, 11 and 12 are expressed as:

$$\begin{aligned} \frac{u_{i,j+1}-u_{i,j}}{\Delta t} - \frac{u_{i+1,j}-u_{i,j}}{\Delta y} = &\left(\frac{u_{i-1,j}-2u_{i,j}+u_{i-1,j}-2u_{i,j+1}+u_{i+1,j+1}}{2(\Delta y)^2}\right)\\ &+Gr\left(\frac{\theta_{i,j+1}-\theta_{i,j}}{2}\right) + Gm\left(\frac{C_{i,j+1}-C_{i,j}}{2}\right)\\ &-\left(M+\frac{1}{K}\right)\left(\frac{u_{i,j+1}+u_{i,j}}{2}\right) \end{aligned} \tag{15}$$

$$\begin{aligned}\frac{\theta_{i,j+1}-\theta_{i,j}}{\Delta t}-\frac{\theta_{i+1,j}-\theta_{i,j}}{\Delta y}=\\ \frac{1}{Pr}\left(1+\frac{4R}{3}\right)\\ \left(\frac{\theta_{i-1,j}-2\theta_{i,j}+\theta_{i-1,j}-2\theta_{i,j+1}+\theta_{i+1,j+1}}{2(\Delta y)^2}\right)+\\ Du\left(\frac{C_{i-1,j}-2C_{i,j}+C_{i-1,j}-2C_{i,j+1}+C_{i+1,j+1}}{2(\Delta y)^2}\right)\end{aligned} \tag{16}$$

$$\begin{aligned}\frac{C_{i,j+1}-C_{i,j}}{\Delta t}-\frac{C_{i+1,j}-C_{i,j}}{\Delta y}=\\ \frac{1}{Sc}\left(\frac{C_{i-1,j}-2C_{i,j}+C_{i-1,j}-2C_{i,j+1}+C_{i+1,j+1}}{2(\Delta y)^2}\right)\\ +Sr\left(\frac{\theta_{i-1,j}-2\theta_{i,j}+\theta_{i-1,j}-2\theta_{i,j+1}+\theta_{i+1,j+1}}{2(\Delta y)^2}\right)\\ -K_r\left(\frac{C_{i,j+1}+C_{i,j}}{2}\right)^2\end{aligned} \tag{17}$$

boundary conditions are also rewritten as:

$$\begin{aligned}u_{i,0}=0 \quad \theta_{i,0}=0 \quad C_{i,0}=0 \quad \forall\, i\\ u_{0,j}=1 \quad \theta_{0,j}=e^{-j\Delta t} \quad C_{0,j}=e^{-j\Delta t}\\ u_{n,j}=0 \quad \theta_{n,j}\to 0 \quad C_{n,j}\to 0\end{aligned} \tag{18}$$

where index i represents to y and j represents to time t, $\Delta t = t_{j+1}-t_j$ and $\Delta y = y_{i+1}-y_i$. Getting the values of u, θ and C at time t , we may compute the values at time $t+\Delta t$ as following method: we substitute $i = 1,2,...,n-1$, where n correspond to ∞ ,equations 15 to 17 give tridiagonal system of equations with boundary conditions in equation 18, are solved employing Thomos algorithm as discussed in Carnahan et al.[11], we find values of θ and C for all values of y at $t+\Delta t$. Equation 15 is solved by same to substitute these values of θ and C, we get solution for u till desired time t.

4. Analysis of Result

The present work analyzes the boundary layer unsteady MHD flow past a porous vertical plate with the Soret-Dufour effect. The influence of the order of chemical reaction has been incorporated in the mass equation. In order to see a physical view of work, numerical results of velocity profile u, temperature profile θ, concentration profile C have been discussed with the help of graphs and skin friction coefficients, Nusselt number and Sherwood number are discussed with the help of tables. The following values are used for investigation $Gr = 5$, $Gm = 5$ and $K = 1$.

The effect of magnetic parameter M on velocity u is depicted in figure 16. It has seen that fluid velocity decreasing with an increase in M. It is noted from figure 7 that increasing radiation parameter R, velocity u increases. This is correct observation because the increase in radiation reveals heat energy to flow. In figure 10, velocity decreases as Prandtl number Pr increases and temperature decreases in figure 11 when Pr increases. In figure 12 concentration C near to plate decreases and some distance from plate concentration increases as Prandtl number increases. Figure 8 depicts the importance of radiation on temperature distribution. It is analyzed that an increase in R, temperature θ increases and it is notable that an increase in R concentration C near to plate decrease after that increases in figure 9.

Figure 6 depicts the variation of Schmidt number Sc as concentration decreases rapidly with increase Sc. It is noteworthy that on increasing Schmidt number Sc temperature profile in figure 5 increases near to plate only while velocity profile in figure 4 decreases near to plate. We demonstrate the influence of Soret number in velocity, temperature and concentration in figure 17, 18 and 19 respectively. It is analyzed that an increase in Sr, velocity u increases; temperature decreases near to plate after then increase and concentration increases rapidly. In figure 13, 14 and 15, it is seen that velocity increases and concentration decreases as increase Dufour number Du whereas temperature increases as Du increases

Figures 1, 3 and 9 depict the behavior of chemical reaction parameter Kr on velocity, temperature and concentration respectively. It is seen that velocity decreases; temperature increases slowly as Kr increases and concentration

decreases rapidly as Kr increase. It is observed from table 1 that M increases, the skin friction coefficient decreases. Change in Schmidt number Sc, Pr and Pr effects as skin friction coefficient and Nusselt number decreases while Sherwood number increases.
Skin friction coefficient and Sherwood number increase whereas Nusselt number decreases when Dufour number Du and radiation parameter R increase. Increase in Soret number Sr, Skin friction and Nusselt number Nu increase while Sherwood number decreases.

5. Conclusion

Effect of second-order chemical reaction, change in Soret-Dufour on unsteady MHD flow past a vertical porous plate immersed in a porous medium are analyzed. This investigation the following conclusions have come:

1. The effect of radiation on concentration is noteworthy. It is observed that increasing values of R, concentration falls down and after some distance from the plate, it goes up slowly-slowly. Interestingly, the same type of change in concentration has been found on increasing Prandtl number Pr.
2. For increasing values of Kr, it is a considerable enhancement in velocity, i.e. velocity decreases slowly.
3. Increasing values of Soret and Dufour number, it is observed that temperature profile in the thermal boundary layer increases whereas temperature profile first decreases after then increases slowly in the boundary layer.
4. Schmidt number greatly influence the concentration profile in the concentration boundary layer.

Acknowledgements

We acknowledge our principal Dr. V. C. Tripathi and chief proctor of science faculty Dr A. K. Dwivedi and thank for encouraging to complete this research work.

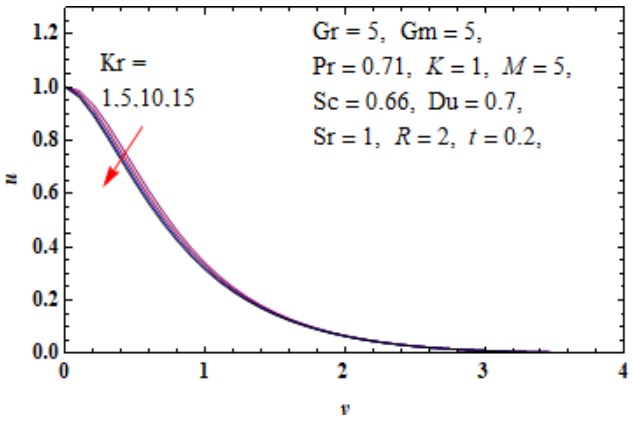

Fig. 1. Velocity Profiles for Different Values of Kr

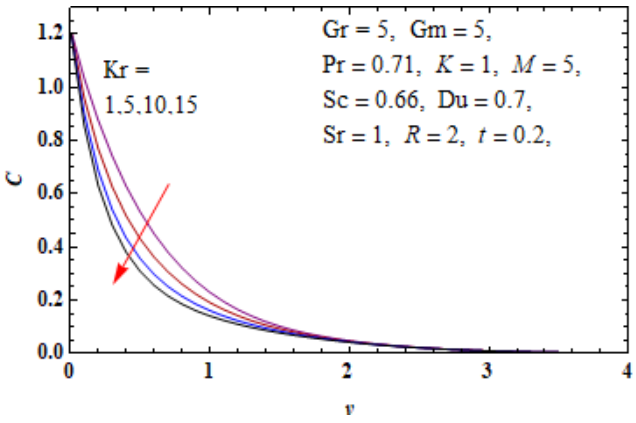

Fig. 2. Concentration Profiles for Different Values of Kr

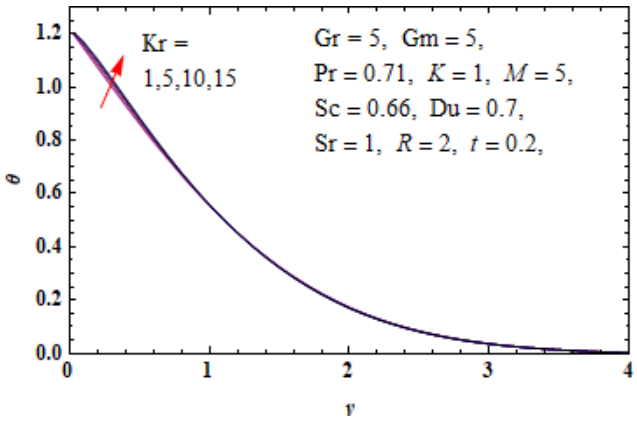

Fig. 3. Temperature Profiles for Different Values of Kr

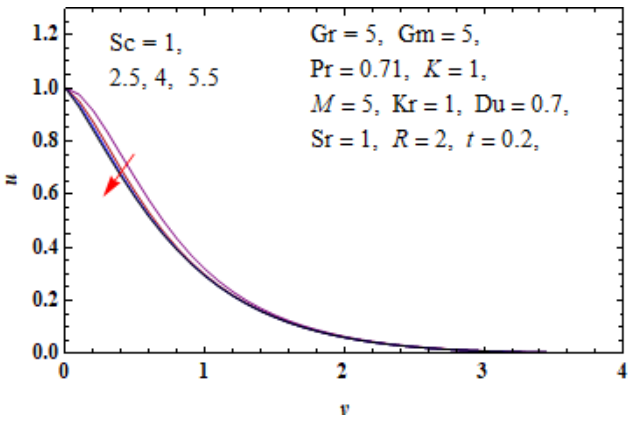

Fig. 4. Velocity Profiles for Different Values of Sc

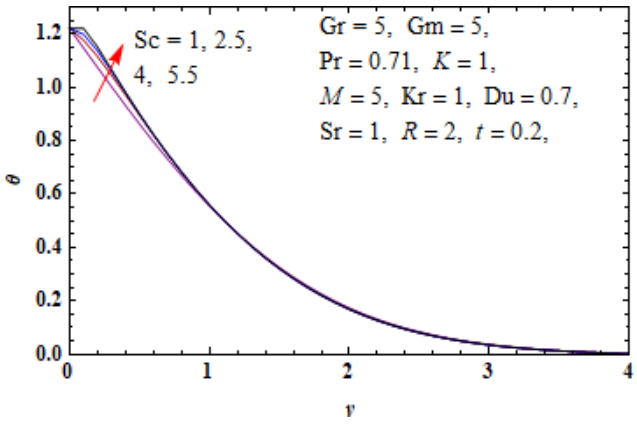

Fig. 5. Temperature Profiles for Different Values of Sc

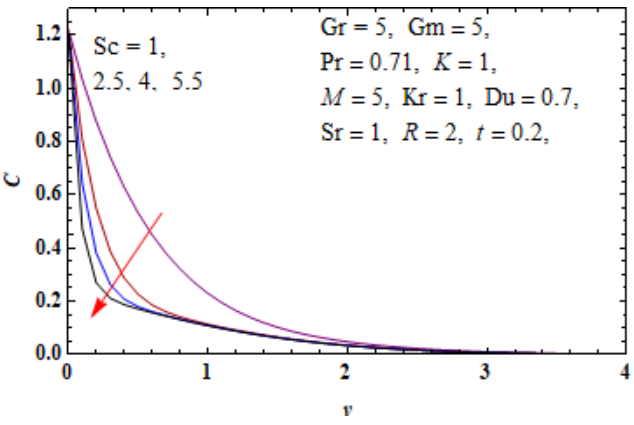

Fig. 6. Concentration Profiles for Different Values of Sc

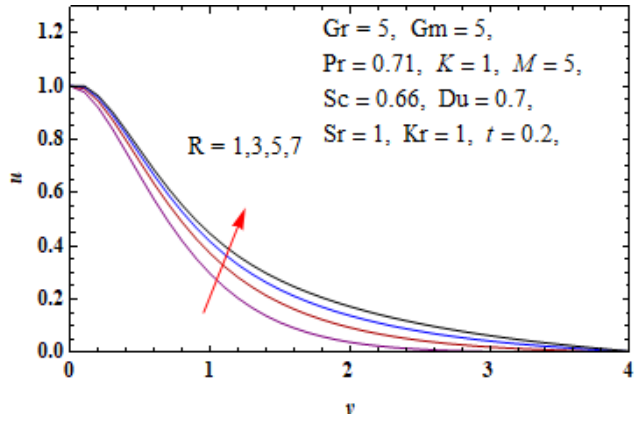

Fig. 7. Velocity Profiles for Different Values of R

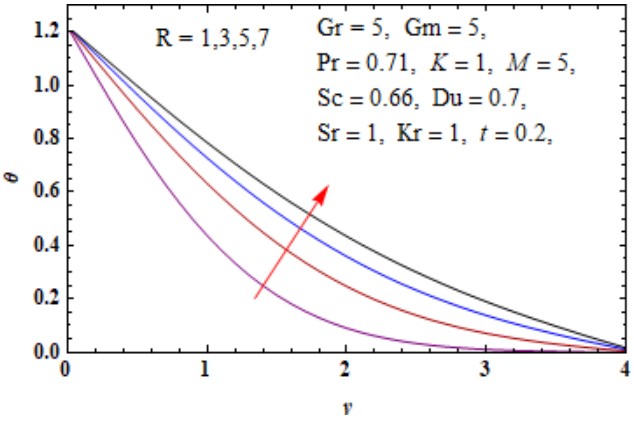

Fig. 8. Temperature Profiles for Different Values of R

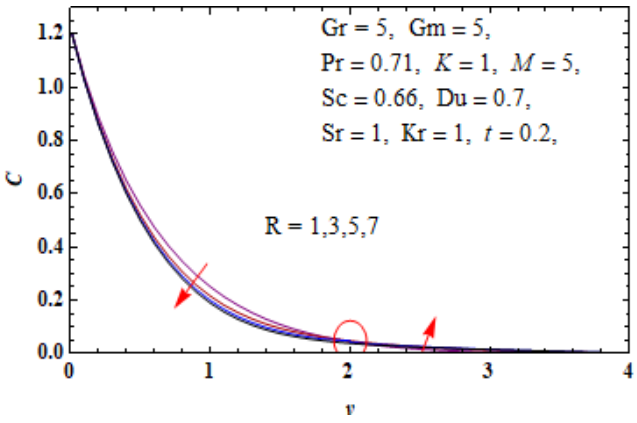

Fig. 9. Concentration Profiles for Different Values of R

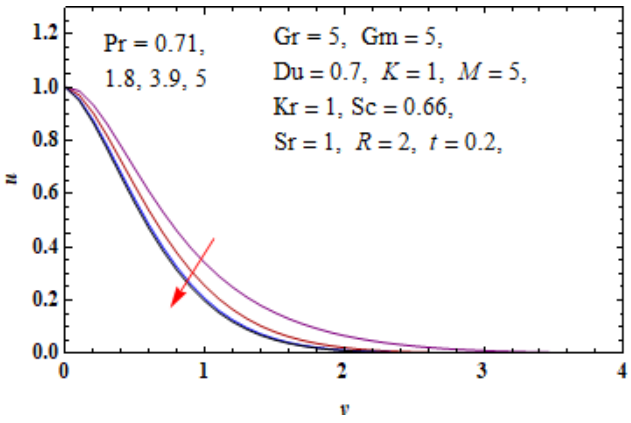

Fig. 10. Velocity Profiles for Different Values of Pr

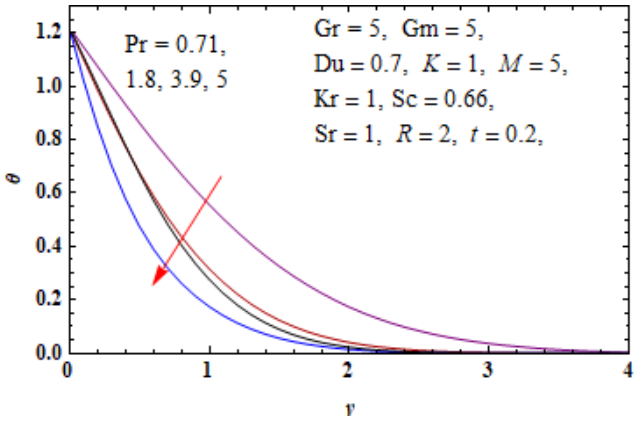

Fig. 11. Temperature Profiles for Different Values of Pr

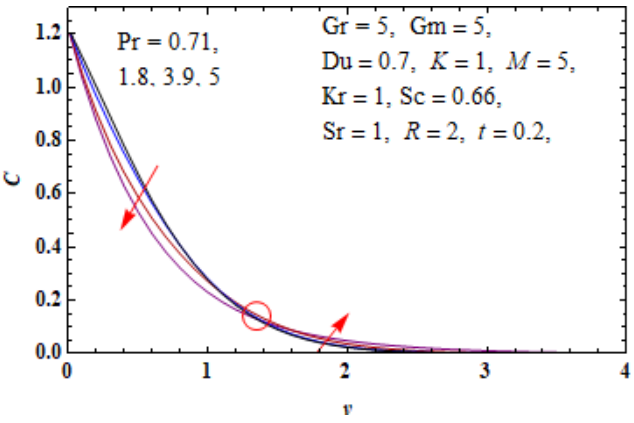

Fig. 12. Velocity Profiles for Different Values of Pr

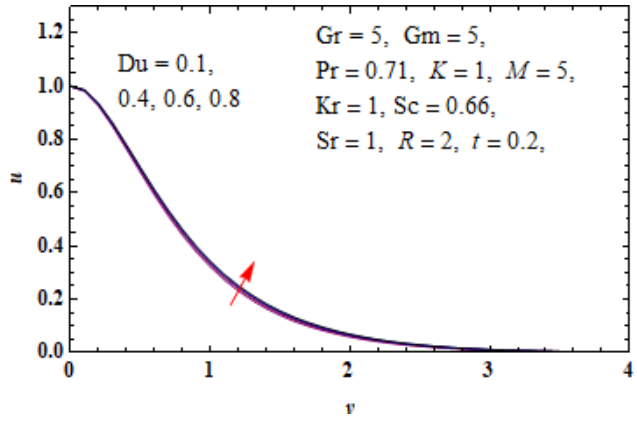

Fig. 13. Velocity Profiles for Different Values of Du

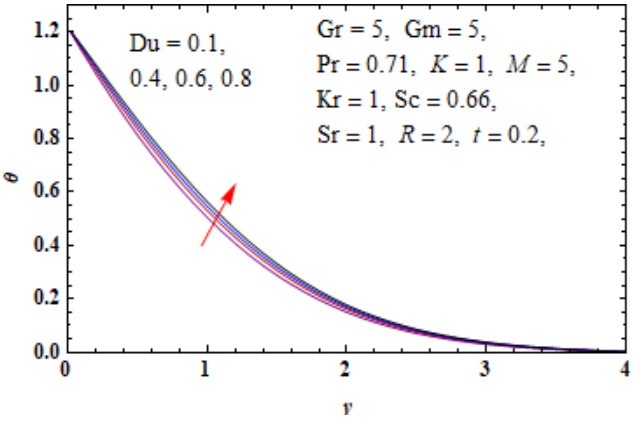

Fig. 14. Temperature Profiles for Different Values of Du

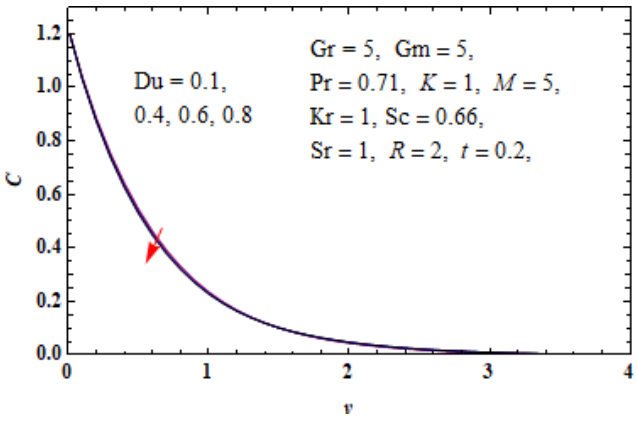

Fig. 15. Concentration Profiles for Different Values of Du

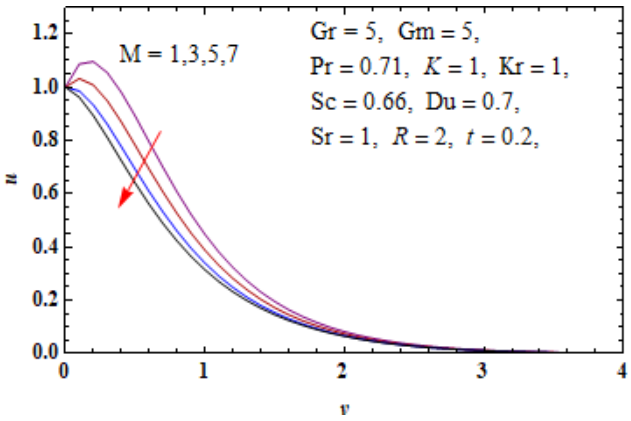

Fig. 16. Velocity Profiles for Different Values of M

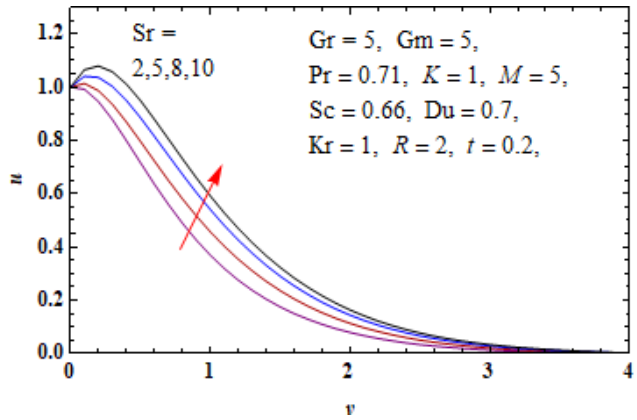

Fig. 17. Velocity Profiles for Different Values of Sr

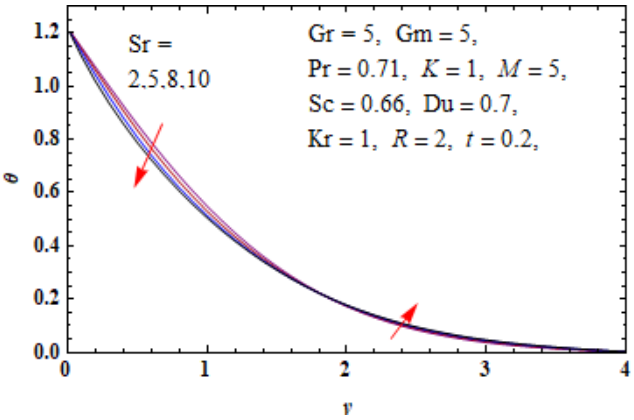

Fig. 18. Temperature Profiles for Different Values of Sr

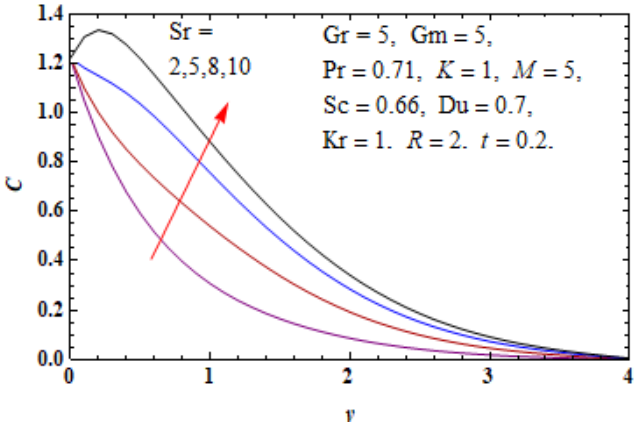

Fig. 19. Concentration Profiles for Different Values of Sr

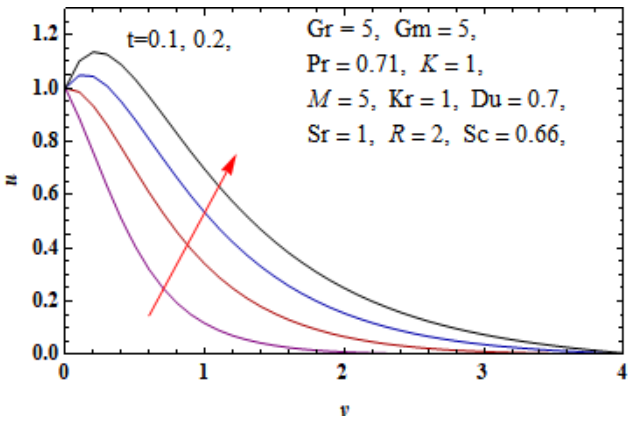

Fig. 20. Velocity Profiles for Different Values of t

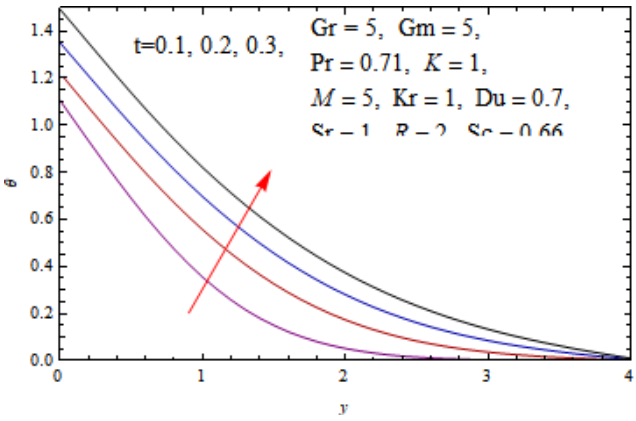

Fig. 21. Temperature Profiles for Different Values of t

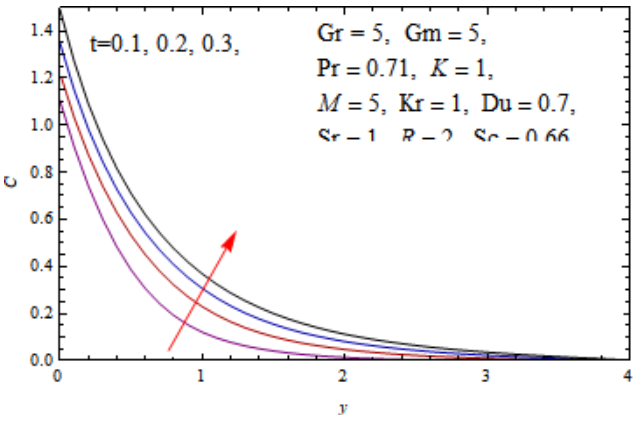

Fig. 22. Concentration Profiles for Different Values of t

Table 1. Skin friction coefficient τ, Nusselt number Nu and Sherwood number Sh for different values of parameters taking fix values of $Gr = 5, Gm = 5, K = 1$

M	Pr	Du	Sc	Sr	R	Kr	t	τ	Nu	Sh
1	0.71	0.7	0.66	1	2	1	0.2	0.864235	0.726639	1.88313
3	0.71	0.7	0.66	1	2	1	0.2	0.322411	0.726639	1.88313
5	0.71	0.7	0.66	1	2	1	0.2	−0.145106	0.726639	1.88313
7	0.71	0.7	0.66	1	2	1	0.2	−0.552673	0.726639	1.88313
5	0.71	0.7	0.66	1	2	1	0.2	−0.145106	0.726639	1.88313
5	1.8	0.7	0.66	1	2	1	0.2	−0.306952	1.17514	1.71535
5	3.9	0.7	0.66	1	2	1	0.2	−0.454595	1.95088	1.3442
5	5	0.7	0.66	1	2	1	0.2	−0.506098	2.44075	1.08101
5	0.71	0.1	0.66	1	2	1	0.2	−0.184158	0.884385	1.81474
5	0.71	0.4	0.66	1	2	1	0.2	−0.164862	0.807443	1.84791
5	0.71	0.6	0.66	1	2	1	0.2	−0.151744	0.754025	1.87115
5	0.71	0.8	0.66	1	2	1	0.2	−0.138415	0.698781	1.89536
5	0.71	0.7	1	1	2	1	0.2	−0.252761	0.66509	2.37381
5	0.71	0.7	2.5	1	2	1	0.2	−0.501107	0.435501	4.15155
5	0.71	0.7	4	1	2	1	0.2	−0.633089	0.219842	5.79444
5	0.71	0.7	5.5	1	2	1	0.2	−0.725482	−0.00660136	7.5098
5	0.71	0.7	0.66	2	2	1	0.2	−0.0793209	0.742261	1.7445
5	0.71	0.7	0.66	5	2	1	0.2	0.138503	0.802023	1.2357
5	0.71	0.7	0.66	8	2	1	0.2	0.407341	0.905335	0.40656
5	0.71	0.7	0.66	10	2	1	0.2	0.650273	1.06935	−0.854984
5	0.71	0.7	0.66	1	1	1	0.2	−0.221572	0.910378	1.82022
5	0.71	0.7	0.66	1	3	1	0.2	−0.0954244	0.625371	1.91363
5	0.71	0.7	0.66	1	5	1	0.2	−0.0312967	0.51042	1.94427
5	0.71	0.7	0.66	1	7	1	0.2	−0.00997082	0.445052	1.96
5	0.71	0.7	0.66	1	2	1	0.2	−0.145106	0.726639	1.88313
5	0.71	0.7	0.66	1	2	5	0.2	−0.242461	0.635327	2.62373
5	0.71	0.7	0.66	1	2	10	0.2	−0.322231	0.559702	3.22481
5	0.71	0.7	0.66	1	2	15	0.2	−0.378286	0.505111	3.65307
5	0.71	0.7	0.66	1	2	1	0.1	−1.12793	0.859204	1.96014
5	0.71	0.7	0.66	1	2	1	0.2	−0.145106	0.726639	1.88313
5	0.71	0.7	0.66	1	2	1	0.3	0.485931	0.699678	2.00198
5	0.71	0.7	0.66	1	2	1	0.4	1.01477	0.707993	2.19963

References

[1] Nadeen S., Akbar N.S., Haq R.U. and Khan Z.H. (2013), Radiation effect on MHD stagnation point flow of nanofluid towards a stretching surface with convective boundary conditions, *Chinese journal of Aeronautics*, 26 (6), 1389–1397.

[2] Ibrahim S.M., Mabood F, Lorenzini G and Lorenzini E. (2017), Radiation effects on Williamson nanofluid flow over a heated surface with magnetohydrodynamics, *International Journal of Heat and Technology*, 35 (1), 196–204.

[3] Oztop H.F. and Selimefendigil F. (2016), Analysis of MHD mixed convection in a flexible walled and nanofluids filled lid driven cavity with volumetric heat generation. *Int J Mech Sci*, 118, 113–124.

[4] Kumar S. and Rajput U.S. (2012), Radiation effect on MHD flow past an impulsively started vertical plate with variable heat and mass transfer, *J. Appl Math. Mech.*, 8, 66–85.

[5] Ahmad A., Hayat T., Hina Z. and Anum T. (2017), Soret and Dufour effects on MHD peristaltic transport of jeffery fluid in a curved channel with convective boundary conditions, *PLOS ONE*, 12 (2).

[6] Katagiri Srihari. (2018), Soret, Dufour and Hall effects on unsteady MHD flow past a semi infinite vertical plate by the presence of heat source, *Journal of international academy of physical sciences*, 22 (1), 25–50.

[7] Kharabela swain, Sampada K. Parida and Gauranga C. Dash. (2019) Higher order chemical reaction on MHD nanofluid flow with slip boundary conditions: A numerical approach, *Mathematical modeling of engineering*, 6 (2), 293–299.

[8] Anjana Matta, Nagaraju Gajjela. (2018), Order of chemical reaction and convective boundary condition effects on micropolar fluid flow over a stretching sheet, *AIP advances*, 8 Article ID 115212.

[9] Halima usman, Ime Jimy Uwanta and Smaila Kanba Ahmad. (2016), Magnetohydrodynamics free convection flow with thermal radiation and chemical reaction effects in presence of variable suction, *MATEC Web of Conferences*, 64, Article ID 01002.

[10] Rahman M. and Dash M. (2012), Combined effects of internal heat generation and higher order chemical reaction on the non-Darcian forced convective flow of a viscous incompressible fluid with variable viscosity and thermal conductivity over a stretching surface embedded in a porous medium, *Can. J. Chem. Eng.*, 90, 1631–1644.

[11] Brice Carnahan, H.A. Luther and James O. Wilkes. (1990), *Applied Numerical Methods*, Krieger Pub Co, Florida.